Strengthening Slender Reinforced Concrete Columns using Bonded CFRP Laminates

Conference Paper · June 2013

CITATION
1

READS
8

2 authors:

Pedram Sadeghian
Dalhousie University
23 PUBLICATIONS **66** CITATIONS
SEE PROFILE

Amir Fam
Queen's University
177 PUBLICATIONS **1,804** CITATIONS
SEE PROFILE

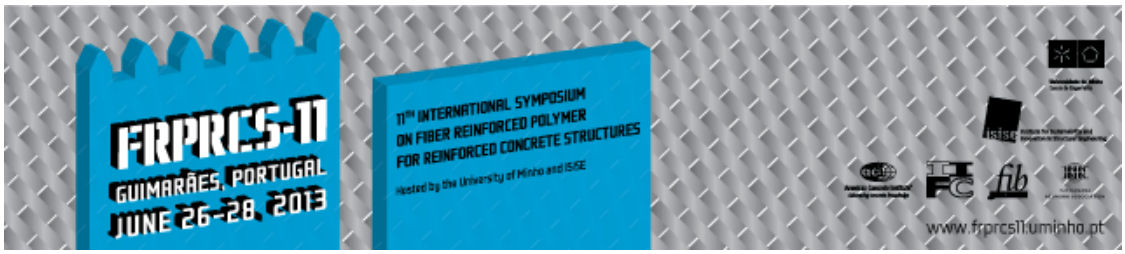

STRENGTHENING SLENDER REINFORCED CONCRETE COLUMNS USING BONDED CFRP LAMINATES

P. Sadeghian[1], A. Fam[2]
[1]Assistant Professor, Penn State Harrisburg, Middletown, PA, USA, pedram@psu.edu
[2]Professor, Queen's University, Kingston, ON, Canada, fam@civil.queensu.ca

Keywords: Analytical analysis; CFRP; Flexural strengthening; Column; Buckling failure.

SUMMARY
Most research on retrofitting reinforced concrete (RC) columns using, fiber reinforced polymer (FRP) materials has focused on the confinement issue of the section. Slender reinforced concrete columns may suffer global buckling failure at loads much lower than their counterpart short columns. This paper addresses the effect of bonding longitudinal carbon FRP (CFRP) plates to the sides of the slender column, in order to enhance its flexural rigidity. This in turn enhances its buckling load according to Euler's buckling rule. The study explored high modulus CFRP plates, which were adhesively bonded to the columns. Also, near surface mounted (NSM) reinforcement were explored using standard-modulus CFRP strips. The study focused on pin-ended columns at this stage, but will be expanded to different boundary conditions. The study showed that significant gains in axial strength can be achieved by reducing the P-Delta effect and hence changing the loading path on the axial load-bending moment interaction curve of the section, leading to interception of the interaction curve at a higher load representing considerable gain in strength. To the author's knowledge, this novel approach has not been explored before for slender RC columns despite its simple concept.

1. INTRODUCTION

In recent years, fiber reinforced polymer (FRP) composites have been very ideal materials for strengthening of existing reinforced concrete (RC) structures. Moreover, strengthening of existing RC columns with FRP composites has been researched by many researchers and practiced by many engineers. So far, it is commonly accepted that applying transverse strengthening systems such as unidirectional FRP wraps on RC columns can effectively provide lateral confinement on concrete core and enhance strength and ductility of the columns under uniaxial compressive loadings [1, 2, 3, 4]. This system is more effective on RC columns with circular cross section in compare to rectangular sections. Transverse FRPs has also been successfully examined for strengthening of RC columns under eccentric compressive loadings [5, 6, 7]. Transverse FRP strengthening systems can enlarge axial load-bending moment (P-M) interaction curves under combination of large axial loads and low bending moments [8, 9].

The effects of combination of transverse and longitudinal fibers on RC columns have been studied by some researchers [10, 11, 12, 13], but their main focus has been on effectiveness of FRPs and P-M interaction curves not on the effects of slenderness. Moreover, in some design guidelines such as ACI 440.2R [14] there is a gap for slender RC columns strengthened with FRPs. Recently, some studies [15, 16] have been conducted on FRP strengthening of slender RC columns, but their concentrations have been on enlarging P-M interaction curves and upgrading of the columns through applying transverse FRPs and increasing confinement.

It has been mainly accepted that longitudinal FRP strengthening systems such longitudinal fabrics, bonded laminates, and near surface mounted (NSM) systems on RC columns can only enlarge P-M interaction curves of the columns under large bending moments and low axial loads and have no significant effect under large axial loads and low bending moments. The effect of longitudinal FRPs on slender RC columns has been neglected based on the lower stiffness of conventional FRPs in compare to steel reinforcements which is very important parameter for second order deformations. But these days, based on the availability of some high modulus carbon FRPs (CFRPs) with elastic modulus up to two times of steel reinforcements, the effect of FRPs on second order deformations can be completely different. This concept has been successfully examined by Shaat and Fam [17] for strengthening of slender steel columns with longitudinal high modulus CFRPs. Thus, same behavior could be expected for slender RC columns.

Figure 1 shows hypothetical performance of a short and slender RC column before and after strengthening with longitudinal high modulus CFRPs. Straight line OA represents loading path related to a typical short RC column under compressive axial load P and eccentricity e_o. Applying longitudinal FRPs on these columns changes failure point A to A' which upgrades load capacity of the columns a little as shown in the figure. Let's consider a slender column with the same cross section, eccentricity, and strengthening system. Because the RC column is slender, lateral deformations are significant and eccentricity at mid height increases extensively based on the concept of second order deformations, which leads to typical non-linear loading path OB with a significant lower load capacity (i.e. failure point B) in compare to short RC column (i.e. failure point A).

The authors expect to change load path OB to OB' by applying high modulus CFRPs in order to upgrade failure point B to B' which represent a significant strengthening gain for slender column in compare to short column. This hypothesis is logical as second order deformations are directly related to flexural stiffness of the slender column and high modulus CFRPs are able to provide enough flexural stiffness to the change loading path. The authors believe that strengthening mechanism with longitudinal FRPs is fundamentally different for short and slender RC columns. For Short columns strengthening gain attains only through enlarging interaction diagram, however for slender columns longitudinal high modulus FRPs are able to change loading path to achieve a significant strengthening gain.

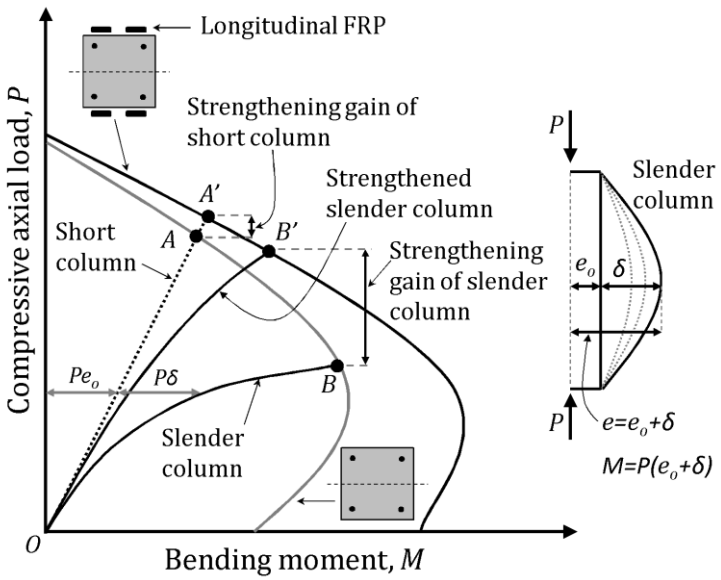

Figure 1: Hypothetical performance of short and slender RC columns before and after strengthening with longitudinal high modulus CFRPs.

While FRP strengthening of short RC columns through applying confinement on concrete have been studied extensively, few studies as mentioned have been conducted on slender RC columns. Moreover, these few studies have been concentrated on strengthening through applying transverse FRPs and increasing confinement to enlarge P-M interaction curve and there is no study to concentrate on changing loading path through applying longitudinal FRPs and increasing flexural stiffness. In this paper, the authors develop an analytical modeling to predict loading path of slender RC columns strengthened with longitudinal high modulus CFRPs. The model is verified with some experimental data on slender RC columns.

2. ANALYTICAL MODELING

The objective of analytical modeling is to predict loading path of slender RC columns strengthened with longitudinal high modulus CFRPs. As shown in Fig. 1, the loading path is nonlinear and its nonlinearity is a function of slenderness ratio or flexural stiffness of column. In general the loading path has two parts of ascending and descending branches with a peak load which is corresponding buckling load. For ordinary slender RC columns with practical slenderness, before reaching the peak load, the ascending branch hits P-M interaction curve of column and material failure as FRP rupture at tension side or concrete crushing at compression side of section happens.

For RC columns with very high slenderness ratio, the ascending branch terminates at the buckling load and load path continues as a descending branch up to hit the interaction curve. This means that for all RC columns with and without buckling, material failure at interaction curve is the end of the story. It should be mentioned that an interaction curve is a function of section geometry and material properties. On the other hand, interaction curve is not a function of slenderness, however after predicting load paths for different eccentricity and slenderness and projecting failure points on linear load path of the corresponding short column, P-M interaction curves of slender columns for different slenderness can be plotted.

In order to plot the load path of a column at given initial eccentricity e_o, an iterative analysis is required (at any given load/displacement level) to capture second order deformation of the column. As shown in Fig. 1, initial bending moment Pe_o creates a lateral deformation δ_o and the lateral deformation δ_o increase eccentricity to $e_o+\delta_o$. The new eccentricity creates an additional bending moment $P\delta_o$ and the additional bending moment creates an additional deformation, and this procedure continues up to reach a convergence at final lateral deformation δ and final bending moment $P(e_o+\delta)$. This iterative procedure should be performed at different load/displacement level to have enough point for plotting the entire load path. The first step in this procedure is cross sectional analysis of a FRP-strengthened RC column to determine internal forces at each load step and have corresponding moment-curvature curve.

2.1 Section Analysis

Figure 2(a) shows a RC column with rectangular cross section (width b × height h) and longitudinal steel rebars at typical tension side with total area As at effective depth d, at mid-section with total area A_{sm} at effective depth d_m (can be 0.5h), and at typical compression side with total area A'_s at effective depth d'. The column is strengthened with longitudinal bonded FRP plates or NSM FRP reinforcements at typical tension side with total area A_f at effective depth d_f and at typical compression side with total area A'_f at effective depth d'_f. The effective depth d'_f for bonded FRP plates is positive and for NSM FRP reinforcements is negative.

It is assumed that strain profile is linear and FRPs and concrete are perfectly bonded without any slip, as shown in Fig. 2(b). Thus, strain at steel rebars (i.e. ε_s, ε_{sm}, and ε'_s) and at FRPs (i.e. ε_f and ε'_f) are proportional with maximum concrete strain ε_c and curvature ψ. The column is under compressive axial load P with eccentricity e (with respect to mid height of concrete section) to create a bending moment about the axis perpendicular to height h, as shown in Fig. 2(c).

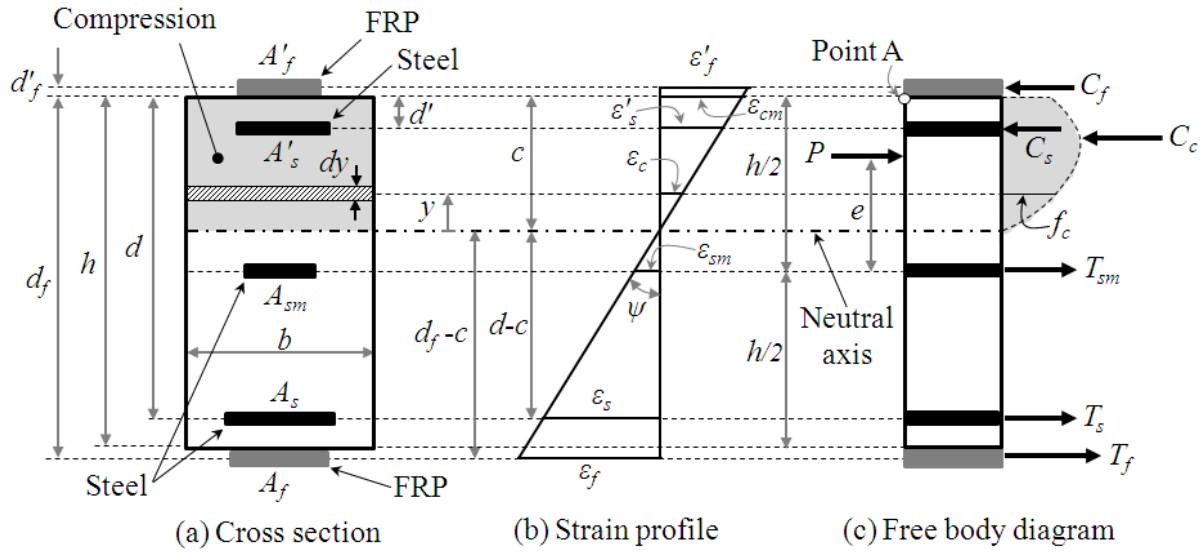

Figure 2: Cross sectional analysis of a FRP-strengthened RC column.

Tensile concrete is neglected and neutral axis depth c is measured from the extreme concrete compression fiber. As there in no transverse FRP for confinement, compressive behavior of concrete can be adequately described by the Popovics model [18]. As shown in Fig. 2, the compressive stress f_c at distance y from the neutral axis, corresponding to a strain ε_c, is given by

$$f_c = \frac{f'_c\left(\varepsilon_c / \varepsilon'_c\right) r}{r - 1 + \left(\varepsilon_c / \varepsilon'_c\right)^r} \tag{1}$$

where f'_c is unconfined concrete strength, ε'_c is corresponding strain, and $r=E_c/(E_c-E_{sec})$. The elastic modulus E_c, secant modulus E_{sec}, and ε'_c are determined as $E_c=4700\sqrt{f'_c}$ in MPa, $E_{sec}=f'_c/\varepsilon'_c$, and $\varepsilon'_c=1.7f'_c/E_c$; respectively. In order to develop P-M interaction curves, maximum useable strain ε_{cu} at extreme concrete compression fiber is assumed equal to 0.003 which is compatible with ACI 318 [19] and ACI 440-2R [14] for unconfined concrete.

The behavior of steel rebars is assumed linear elastic-perfectly plastic with elastic modulus E_s, yielding stress f_{sy}, and yielding strain ε_{sy}. The behavior of FRPs is assumed linear elastic with elastic modulus E_f up to tensile rupture stress f_{ftu} (tensile rupture strain ε_{ftu}) and compressive crushing stress f_{fcu} (compressive crushing strain ε_{fcu}). Based on Fig. 2(b), strain ε_c at any concrete compression fiber is evaluated as $\varepsilon_c=\psi.y$ and strain ε_{cm} at extreme concrete compression fiber (i.e. at $y=c$) is evaluated as $\varepsilon_{cm}=\psi.c$. Thus, resultant force C_c and resultant moment M_c corresponding to compressive concrete can be expressed as the following:

$$C_c = b\int_a^c f_c\,dy \tag{2}$$

$$M_c = b\int_a^c (c-y)\, f_c\,dy \tag{3}$$

where a is zero when neutral axis is inside of concrete section and is $\psi(c-h)$ when neutral axis is outside. As shown in Fig. 2(c), all moments are taken about point A at extreme concrete compression fiber. For steel rebars, strain ε_s, ε_{sm}, and ε'_s are evaluated as $\varepsilon_s=\psi.(d-c)$, $\varepsilon_{sm}=\psi.(d_m-c)$, and $\varepsilon'_s=\psi.(c-d')$,

respectively. Thus, resultant forces T_s, T_{sm}, and C_s corresponding to typical tensile, mid-section, and typical compressive steel rebars can be expressed as the following:

$$T_s = \begin{cases} E_s\varepsilon_s, & -\varepsilon_{sy} \le \varepsilon_s \le \varepsilon_{sy} \\ f_{sy}A_s, & \varepsilon_{sy} \le \varepsilon_s \\ -f_{sy}A_s, & \varepsilon_s \le -\varepsilon_{sy} \end{cases} \quad (4)$$

$$T_{sm} = \begin{cases} E_s\varepsilon_{sm}, & -\varepsilon_{sy} \le \varepsilon_{sm} \le \varepsilon_{sy} \\ f_{sy}A_{sm}, & \varepsilon_{sy} \le \varepsilon_{sm} \\ -f_{sy}A_{sm}, & \varepsilon_{sm} \le -\varepsilon_{sy} \end{cases} \quad (5)$$

$$C_s = \begin{cases} E_s\varepsilon'_s, & -\varepsilon_y \le \varepsilon'_s \le \varepsilon_y \\ f_yA'_s, & \varepsilon_y \le \varepsilon'_s \\ -f_yA'_s, & \varepsilon'_s \le -\varepsilon_y \end{cases} \quad (6)$$

For FRPs, strain ε_f and ε'_f are evaluated as $\varepsilon_f=\psi.(d_f-c)$ and $\varepsilon'_f=\psi.(c+ d'_f)$, respectively. Thus, resultant forces T_f and C_f corresponding to typical tensile and compressive FRPs can be expressed as the following:

$$T_f = E_f\varepsilon_f A_f \quad (7)$$

$$C_f = E_f\varepsilon'_f A'_f \quad (8)$$

To this end, the internal forces have been expressed in terms of two main parameters, namely curvature ψ and neutral axis depth c. By applying static equilibrium conditions, considering internal and external forces, as shown in Fig. 2(c), the following two equations are derived:

$$C_c + C_s + C_f - T_s - T_{sm} - T_f = P \quad (9)$$

$$M_c + C_s(d') - T_s(d) - T_{sm}(d_m) - T_f(d_f) - C_f(d'_f) = P(0.5h - e) \quad (10)$$

For a given eccentricity e and load P, Equations (9) and (10) are insufficient to obtain the two unknown parameters (i.e. curvature ψ and neutral axis depth c), using a conventional computer program. The results can be used for the lateral deformation calculations of slender RC columns through an iterative analysis which is discussed in the next section.

2.2 Iterative Analysis of Slender Columns

For a slender column under eccentric compressive load, eccentricity e for each section along the column is different than initial eccentricity e_o. Distribution of eccentricity e is a function of lateral deformation of the column. As the lateral deformation is a function of eccentricity as well, an iterative analysis is needed. Let's consider a RC column with length L under symmetric bending, as half of the column shown in Fig. 3.

There is no deformation at point A and Point M is located at mid height with maximum deformation, thus tangent on deformed shape of the column at point M is parallel to original shape of the column. Using Moment-Area method for a point X at a variable distance x from point A, deformation δ_X at point X is expressed as $\delta_X=x.\theta_A-t_{X/A}$. Based on Figure 3, slop at point A (i.e. θ_A) and vertical deviation of tangent at A about point X (i.e. $t_{X/A}$) can be expressed as the following:

$$\theta_A = \int_0^{L/2} \psi(z)dz \quad (11)$$

$$t_{X/A} = \int_0^x \psi(z)(x-z)dz \tag{12}$$

Thus, deformation δ_X as a function of position x is expressed as:

$$\delta_X = x\int_0^{L/2} \psi(z)dz - \int_0^x \psi(z)(x-z)dz \tag{13}$$

In order to converting Equation (13) from a continuous function to a discrete function, the column with length L is equally divided to n number of segments with segment length of $\Delta x=L/n$, as shown in Fig. 3. Thus, deformation δ_i at position x_i (i.e. node number i with curvature ψ_i) can be expressed as the following:

$$\delta_i = x_i\left[\sum_{j=1}^{n/2}\left(\frac{\psi_j+\psi_{j-1}}{2}\right)\Delta x\right] - \left[\sum_{j=1}^{i}\left(\frac{\psi_j+\psi_{j-1}}{2}\right)\left(x_i - x_j + \frac{\Delta x}{2}\right)\Delta x\right] \tag{14}$$

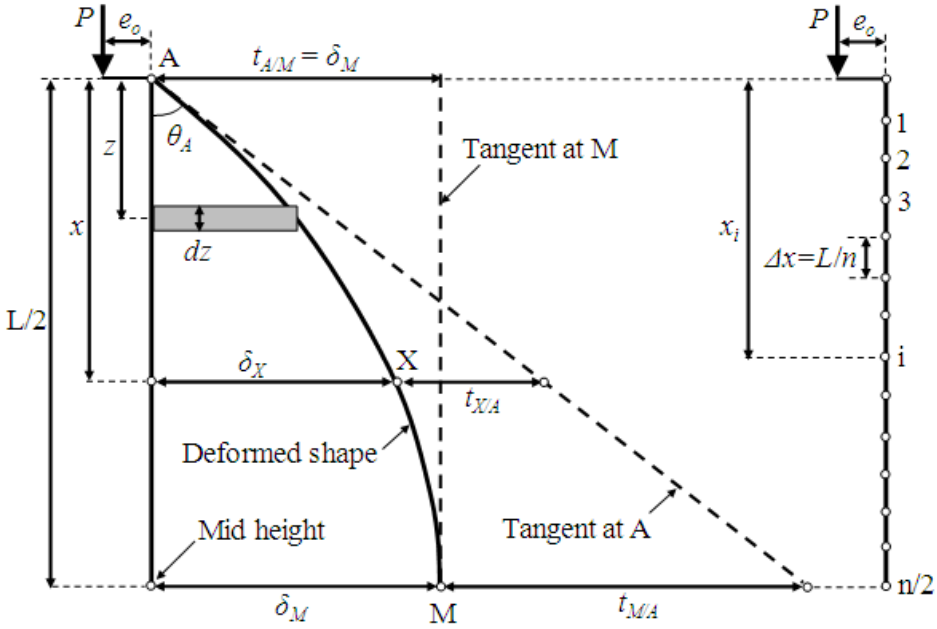

Figure 3: Deformation calculation.

For a given section with axial load P and initial eccentricity e_o, in the first iteration curvature at all nodes is the same, because eccentricity at all nodes is the same. Using Equation (14), deformation at each node can be calculated. In the second iteration, eccentricity at each node is equal to initial eccentricity e_o plus the corresponding deformation δ_i. Thus at each node a new section analysis (as presented in previous section) with new eccentricity $e_o+\delta_i$ can be performed to calculate a new curvature ψ_i. Now, using Equation (14), new deformations can be calculated for the third iteration. This iterative analysis is continued up to reach a convergence which is defined a deformation increment equal to 0.01 mm.

A typical load path of a slender column has two branches of ascending and descending with a pick load. For ascending branch, a load control approach is implemented to determine deformed shape of slender column and corresponding eccentricities for a given axial load level up to the pick load. For the loads close to the pick load, load steps should be refined to have enough points to plot the details of the curve and to capture the peak load. For very slender RC columns, the peak point locates inside of P-M interaction curve, which is corresponding to buckling failure of the columns, but the load path

continues as a descending branch to hit P-M interaction curve for material failure. For conventional slender RC columns, the peak point does not reach as material failure happens before buckling failure. For some conventional slender RC columns under high eccentricity, a peak point may reach just before hitting P-M interaction curve, where yielding of tensile steel rebars can reduce stiffness of column and trigger a buckling failure. In these cases, after a sharp-shape peak point, a short descending branch appears up to hit P-M interaction curve.

Descending branch of load path should be captured using a displacement control approach. The analysis is almost similar to ascending branch, but instead of looking for deformation under a given load, main unknown parameter is load for a given deformation at mid-height of column. It should be mentioned that post buckling behavior of very slender RC columns is not the main subject of this study. Moreover, second order analysis of a RC column using displacement control approach is time consuming. Thus, in order to prevent unnecessary calculations, a sign-shape deformation at descending branch is assumed for a pined RC column as suggested by Lloyd and Rangan [20] and Claeson and Gylltoft [21] for RC columns and verified by Sadeghian et al. [12] for FRP-strengthened RC columns.

3. VERIFICATION

The proposed analytical model is verified with two experimental works on slender columns. The first experimental work was performed by Kim and Yank [22] on conventional slender RC columns, where a series of tests was carried out for 30 tied RC columns with an 80 mm square cross section and three slenderness ratios (λ) of 10, 60 and 100. Three different concrete strengths of 25.5, 63.5, and 86.2 MPa, and two different longitudinal steel ratios of 1.98 and 3.95% were used. The boundary conditions at the ends were both hinged and end eccentricities of 24 mm were equal and of the same sign. Fig. 4 shows interaction diagrams the specimens with concrete strengths of 25.5 MPa and two different longitudinal steel ratios of 1.98 and 3.95%. Experimental load paths are plotted for different slender ness ratios, where the majority of them contain the results of two test specimens. The specimens have been analyzed with the proposed analytical model, as their load paths shown with continuous curves in Fig. 4. It shows that the proposed analytical model is perfectly able to predict the behavior of the experimental columns.

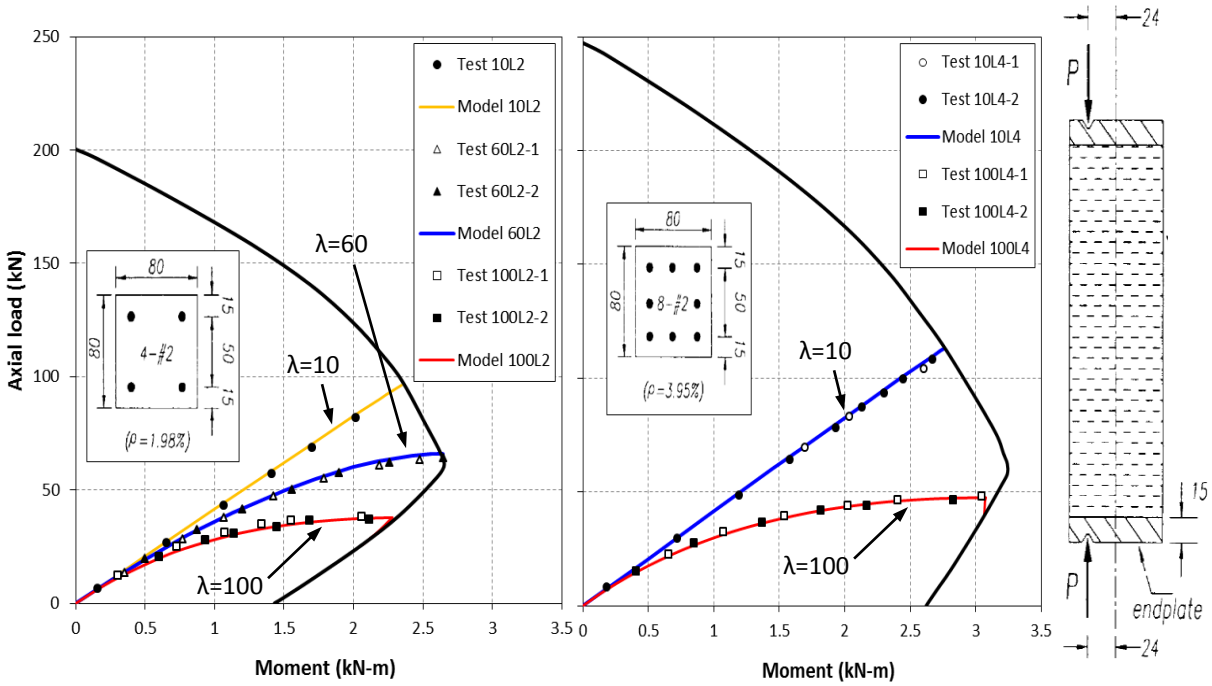

Figure 4: Model verification with experimental data by Kim and Yank [22] on conventional slender RC columns (dimensions in mm).

The second experimental work was performed by Gajdosova and Bilcik [23] on slender RC columns strengthened with longitudinal NSM CFRPs. It should be mentioned that this work is the only available experimental research on slender RC columns strengthened with longitudinal FRPs. The experimental investigation was performed on full-scale slender rectangular RC columns. Columns were divided into four series: non-strengthened columns, columns strengthened by longitudinal NSM CFRP strips, transverse CFRP sheet wrapping, and a combination of these two methods. All columns, as shown in Fig. 5, were 4.1m long with cross-section of 210 × 150 mm. Reinforcement of a column consisted of 8 bars of diameter 10 mm in longitudinal direction and stirrups of diameter 6 mm in distances 150 mm, concerned by up to 30 mm in the heads of a column. Columns were hinge supported at both ends, where the initial end eccentricity (e_o) 40 mm was put into by these supports. At this eccentricity, columns were loaded by a compression force, value of which was growing continuously step by step to the failure.

Among the four specimens, only one specimen with longitudinal NSM CFRP strips is compatible with the framework of the proposed analytical model. For this column, as shown in Fig. 5, three grooves (3 × 15mm) on each longer side of cross-section were cut over the whole length of a column. After cleaning, the grooves were filled with epoxy adhesive and CFRP strips (1.4 × 10mm) were pushed into them. Fig. 5 shows the comparison of the test data and prediction of the proposed analytical model, which have good agreement. The model predicts a little low, which is conservative.

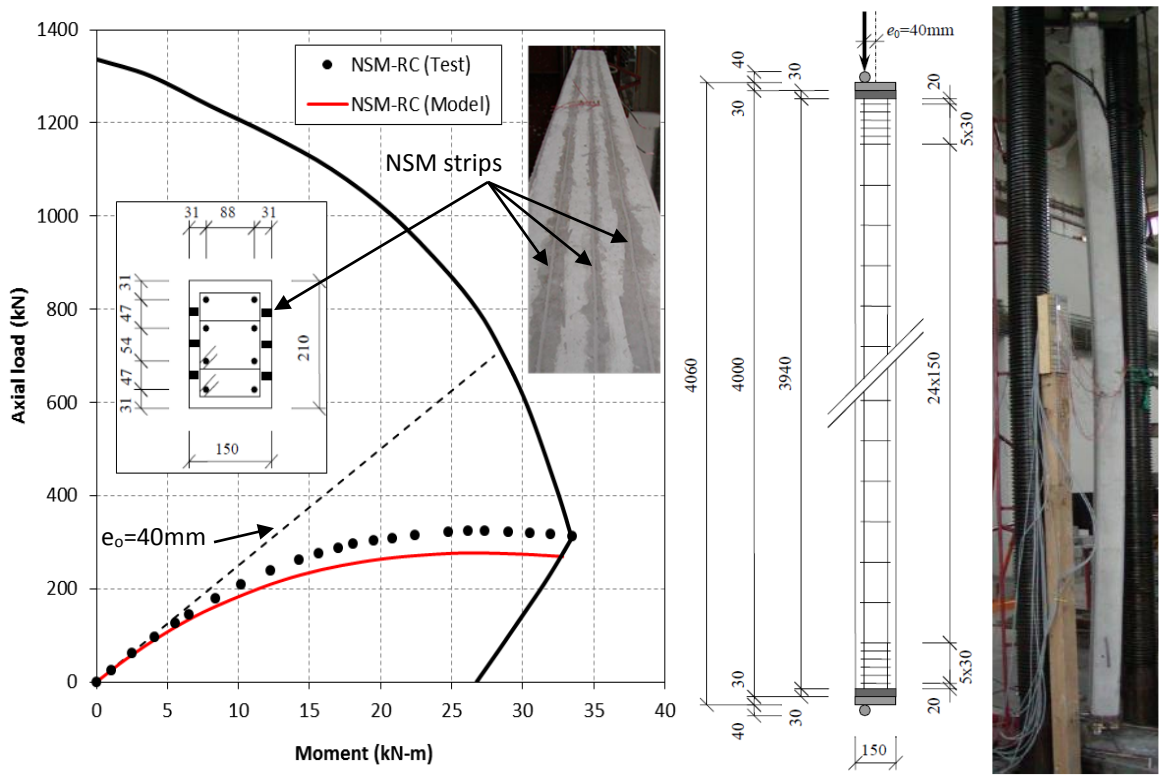

Figure 5: Model verification with experimental data by Gajdosova and Bilcik [23] on slender RC columns strengthened with longitudinal NSM CFRPs.

This analytical research is an ongoing research program. A parametric analysis is performing on parameters such as slenderness ratio, FRP ratio, FRP modulus, FRP strength, and concrete strength. At the end, a design oriented formula will be proposed and verified with the analytical model for practical design applications, which will be presented later.

4. CONCLUSIONS

Transverse FRPs has been successfully examined for strengthening of existing RC columns under eccentric compressive loadings, although main focus has been on effectiveness of FRPs to enlarge interaction curves not on the effects of slenderness and changing load path. In this paper, an analytical model was developed to predict the behavior and load path of slender RC columns strengthened with longitudinal high modulus CFRP reinforcements. The reinforcements can be either bonded strips or NSM bars/strips. In order to predict the load path of a column at a given initial eccentricity, an iterative analysis was employed at any given load/displacement level to capture second order deformation of the column. A typical load path of a slender column has two branches of ascending and descending with a pick load. For ascending branch, a load control approach was implemented to determine deformed shape of slender column and corresponding eccentricities for a given axial load level up to the pick load. As the majority of conventional slender RC columns do not experience a long descending branch, an approximated approach based on a sign-shape deformation was adopted to save processing time. The proposed analytical model was verified with two experimental works on conventional slender RC columns and on slender RC columns strengthened with longitudinal NSM CFRPs. For both cases, the model was able to predict load paths of all experimental specimen very well. A parametric analysis is performing on parameters such as slenderness ratio, FRP ratio, FRP modulus, FRP strength, and concrete strength. At the end, a design oriented formula will be proposed and verified with the analytical model for practical design applications, which will be presented later.

ACKNOWLEDGMENTS

The authors wish to acknowledge the financial support provided by the Ontario Ministry of Research and Innovation (MRI) and Queen's University, through the Postdoctoral Fellowship provided to the first author and the Early Researcher Award and the Chancellor's Research Award provided to the second author.

REFERENCES

[1] Shahawy, M., Mirmiran, A., and Beitelman, A. (2000). "Test and modeling of carbon-wrapped concrete columns." *Composites Part B: Engineering*, 31(6-7), 471–480.
[2] Pessiki, S., Harries, K. A., Kestner, J., Sause, R., and Ricles, J. M. (2001). "The axial behavior of concrete confined with fiber reinforced composite jackets." *Journal of Composites for Construction*, 5(4), 237–245.
[3] Lam, L., and Teng, J. G. (2003). "Design-oriented stress-strain model for FRP-confined concrete." *Construction and Building Materials*, 17(6-7), 471–489.
[4] Mandal, S., Hoskin, A., and Fam, A. (2005). "Influence of concrete strength on confinement effectiveness of fiber-reinforced polymer circular jackets." *ACI Structural Journal*, 102(3), 383–392.
[5] Parvin, A., and Wang, W. (2001). "Behaviour of FRP jacketed concrete columns under eccentric loading." *Journal of Composites for Construction*, 5(3), 146–152.
[6] Li, J., and Hadi, M. N. S. (2003). "Behaviour of externally confined high strength concrete columns under eccentric loading." *Composite Structure*, 62(2), 145–153.
[7] Hadi, M. N. S. (2007). "Behaviour of FRP strengthened concrete columns under eccentric compression loading." *Composite Structure*, 77(1), 92–96.
[8] Saadatmanesh, H., Ehsani, M. R., and Li, M. W. (1994). "Strength and ductility of concrete columns externally reinforced with fiber composite straps." *ACI Structural Journal*, 91(4), 434–447.
[9] Bisby, L., and Ranger, M. (2010). "Axial–flexural interaction in circular FRP-confined reinforced concrete columns." *Construction and Building Materials*, 24(9).1672–1681.
[10] Chaallal, O., and Shahawy, M. (2000). "Performance of fiber-reinforced polymer-wrapped reinforced concrete column under combined axial-flexural loading." *ACI Structural Journal*, 97(4), 659–688.
[11] Fam, A., Flisak, B., and Rizkalla, S. (2003). "Experimental and analytical modeling of concrete-filled fiber-reinforced polymer tubes subjected to combined bending and axial loads." *ACI Structural Journal*, 100(4), 1–11.

[12] Sadeghian, P., Rahai A. R., and Ehsani, M. R. (2010). "Experimental study of rectangular RC columns strengthened with CFRP composites under eccentric loading." *Journal of Composites for Construction*, 14(4), 443–450.
[13] Quiertant, M., and Clement, J. L. (2011). "Behavior of RC columns strengthened with different CFRP systems under eccentric loading." *Construction and Building Materials*, 25(2), 452–460.
[14] ACI 440.2R (2008). "Guide for the design and construction of externally bonded FRP systems for strengthening concrete structures." American Concrete Institute, Farmington, MI.
[15] Fitzwilliam, J., and Bisby L. A. (2010). "Slenderness effects on circular CFRP confined reinforced concrete columns." *Journal of Composites for Construction*, 14(3), 280–288.
[16] Jiang, T., and Teng, J. G. (2011). "Theoretical model for slender FRP-confined circular RC columns." *Construction and Building Materials*, Jiang, T., & Teng, J. G. (2012). Theoretical model for slender FRP-confined circular RC columns. Construction and Building Materials, 32, 66-76.
[17] Shaat, A., and Fam, A. (2009). "Slender steel columns strengthened using high-modulus CFRP plates for buckling control." *Journal of Composites for Construction*, 13(1), 2–12.
[18] Popovics, S. (1973). "A numerical approach to the complete stress-strain curve of concrete." *Cement and Concrete Research*, 3(5), 583–599.
[19] ACI 318 (2011). "Building code requirements for structural concrete." American Concrete Institute, Farmington, MI.
[20] Lloyd, N. A., and Rangan, B. V. (1996). "Studies on high-strength concrete columns under eccentric compression." *ACI Structural Journal*, 93(6), 631–638.
[21] Claeson, C., and Gylltoft, K. (1998). "Slender high-strength concrete columns subjected to eccentric loading." *Journal of Structural Engineering*, 124(3), 233–240.
[22] Kim, J. K., and Yang, J. K. (1995). "Buckling behaviour of slender high-strength concrete columns." *Engineering Structures*, 17(1), 39-51.
[23] Gajdosova, K., and Bilcik, J. (2012). "Slender rectangular concrete columns strengthened by CFRP confinement and NSMR." 6th International Conference on FRP Composites in Civil Engineering CICE 2012, Rome, Italy, 13-15 June 2012.